

Radiometric analysis of isotherms and thermodynamic parameters for cadmium(II) adsorption from aqueous medium by calcium alginate beads

Kangkana Sarkar¹ · Kamalika Sen¹ · Susanta Lahiri²

Received: 14 January 2017 / Published online: 3 March 2017
© Akadémiai Kiadó, Budapest, Hungary 2017

Abstract Studies on the extraction behavior and immobilization of cadmium by greener reagents have important bearings in today's science. No-carrier-added (NCA), ¹⁰⁹Cd radionuclide is a potential candidate towards radiopharmaceutical studies for both in vivo and in vitro applications and is also used in industrial and environmental studies. Herein, we have studied the adsorption and desorption characteristics of cadmium in both NCA and bulk concentrations into calcium alginate using radiochemical method. Various isotherms like Langmuir, Freundlich, Temkin and Dubinin–Radushkevich have been studied and compared to match the adsorption phenomenon. A spontaneous endothermic physisorption process is expected from thermodynamic parameters.

Keywords NCA ¹⁰⁹Cd · Radiopharmaceutical · Calcium alginate · Adsorption · Isotherm model · Thermodynamic parameters

Introduction

No-carrier-added (NCA) radioisotopes are of immense importance for in vivo and in vitro studies owing to their high specific activity and high degree of sensitivity towards various physiological systems. In addition, NCA Cd radionuclides are also regularly employed in material

research, environmental studies, industrial analysis and other fields. ^{111m}Cd ($T_{1/2} = 49$ min) was used long back as a radioactive source in perturbed angular correlation studies with biomolecules like DNA [1]. Recently, similar studies have also been reported for the interactions of ^{111m}Cd with complex molecular assemblies like fullerene [2]. On the other hand, ¹⁰⁹Cd is a common radiotracer for environmental study of Cd pollution. It also has biomedical applications in monitoring long term metabolic activity of cadmium at subcellular and molecular level for its suitable half-life ($T_{1/2} = 462.6$ days) [3]. Several experiments with short lived ¹⁰⁷Cd ($T_{1/2} = 6.5$ h) radionuclide are reported [4–6] which find applications in nuclear medicine when used as ¹⁰⁷Cd/^{107m}Ag ($T_{1/2} = 44.3$ s) generator system [7]. Applications of other radioisotopes of Cd viz., ¹¹¹Cd–¹¹³Cd, ^{114/110}Cd can also be found in the field of analytical and geological sciences [8, 9]. Numerous industrial applications of Cd including rechargeable nickel–cadmium batteries [10], electroplating [11], nuclear fission [12], petroleum industry [13, 14] are also reported in literature.

Besides all these industrial and medical use of cadmium, everyday chunks of cadmium compounds are dumped in municipal dumping ground or thrown to public sewage which is a big threat to the environment as cadmium is a potential carcinogen and accumulates in the human body through food chain affecting the function of kidneys, lungs, bones and other organs [15]. It is also a main constituent of polluted air as particulate matter due to its extreme toxic effect which causes acute and chronic health problems such as bronchial and pulmonary irritation of lung, long term damage of the kidneys, liver, bones, immune system, blood, and nervous system [16–18]. Therefore, studies on immobilization of cadmium and its extraction behavior have important bearings in today's science.

✉ Kamalika Sen
kamalchem.roy@gmail.com

¹ Department of Chemistry, University of Calcutta, 92 APC Road, Kolkata 700009, India

² Chemical Sciences Division, Saha Institute of Nuclear Physics, 1/AF Bidhannagar, Kolkata 700064, India

Present work is a report on the study of adsorption characteristics of ^{109}Cd into a polymeric microporous hydrogel, calcium alginate (CA) through radiochemical method at different conditions. CA beads can be used for the oral treatment for removal of Cd poisoning due to its versatile adsorption properties together with biodegradability, biocompatibility and non-toxicity. Owing to their internal structure, several metal ions can be efficiently trapped in the cage like structure [19–21]. Again CA beads are enormously used towards tissue engineering as well as designing wound dressing material due to their mucoadhesion and bioadhesion characteristics [22]. So it could be suitable in both ways for recovery of skin ailment as well as for remediation of Cd poisoning from the wounded site if designed properly. Adsorption isotherms (Langmuir, Freundlich, Temkin and Dubinin–Radushkevich) were investigated at different temperatures using different concentrations of cadmium (0.1–50 ppm in 10^{-4} M HNO_3) spiked with ^{109}Cd ($T_{1/2} = 1.2665$ a) radioisotope and hence, production and separation of ^{109}Cd was a foremost mission for the aforesaid purpose.

Enormous production route of NCA ^{109}Cd from natural Ag target are reported in the literature [23–25]. The aforementioned articles described several extraction methods of ^{109}Cd by ion-exchange chromatography using Dowex and Aminex, co-precipitation method, liquid–liquid extractions (LLX) using trioctyl amine (TOA) and di-(2-ethylhexyl)phosphoric acid (HDEHP), solvent extraction, aqueous biphasic system (ABS), ABS using room temperature ionic liquid (RTIL) and so on. In all the above methods except ABS, NCA $^{107,109}\text{Cd}$ were separated using many organic solvents/reagents like pyridine, naphthyl substituted thiourea, cyclohexane, chloroform, etc., of which, many are carcinogenic as well as environmentally hazardous. So a greener alternative was searched for the adsorption and accumulation of the said radioisotope.

In the present article, we produced ^{109}Cd following $^{\text{nat}}\text{Ag}(\alpha, \text{pxn})^{109}\text{Cd}$ reaction and separated it from the bulk silver target by simple classical precipitation method. The adsorption studies of NCA ^{109}Cd into CA beads were performed and the adsorption isotherms were evaluated at different temperatures and different Cd concentrations with NCA ^{109}Cd spiked solutions using radiometric method. To the best of our knowledge, this is the first report on radiometric adsorption isotherm analysis of Cd^{2+} onto calcium alginate using NCA radionuclide.

Experimental

CA bead preparation

CA beads were prepared by drop wise addition of 3% (w/v) sodium alginate (Sisco Research Laboratories Pvt. Ltd.)

solution from a burette into 20% w/v calcium chloride dehydrate (Merck, India) solution maintaining the temperature at ~ 4 °C with constant stirring using a magnetic stirrer [26–28]. The beads were kept overnight in the mother liquor and then washed with deionized water prior to their use in the experiment.

Irradiation

A natural silver foil of thickness 2.8 mg/cm^2 was irradiated by 30 MeV α -particles for 7.25 h with an average beam current of $15.48 \mu\text{A}$ at the Variable Energy Cyclotron Centre, Kolkata, India. The total current was measured with the help of an electron suppressed Faraday cup placed at the rear side of the target holder flange. At the end of bombardment (EOB), the target was taken out and cooled for 2 days, and assayed by a CANBERRA p-type high purity germanium (HPGe) detector with a resolution of 2.3 keV at 1.33 MeV in conjunction with DSA 1000 and Genie 2000 software was used for γ -ray spectrometric analysis. ^{111}In (2.8 days), ^{109}Cd (462.4 days) and $^{106\text{m}}\text{Ag}$ (8.28 days) radionuclides were detected in the target matrix. The target was allowed for a complete decay of ^{111}In for 90 days. The $^{106\text{m}}\text{Ag}$ also decayed out during this period and hence the target contained only ^{109}Cd radioisotope in bulk Ag matrix. The energy and the efficiency calibration of the detector was performed using standard sources of known activity such as ^{152}Eu (13.528 a), ^{133}Ba (10.551 a), ^{137}Cs (30.08 a) and ^{60}Co (5.27 a).

Dissolution and separation of bulk silver

The α -irradiated silver target was dissolved in minimum volume of conc. HNO_3 medium. To monitor the fate of bulk Ag in the radiochemical separations it was spiked with a solution of $^{110\text{m}}\text{Ag}$ (249.79 days) prepared in 0.1 M HNO_3 . The $^{110\text{m}}\text{Ag}$ was procured from the Board of Radiation and Isotope Technology (BRIT), India. The solution was evaporated to dryness thrice and was finally taken in 10^{-2} M HNO_3 . A 10 mL active stock solution containing NCA ^{109}Cd and bulk Ag spiked with $^{110\text{m}}\text{Ag}$ was then prepared for radiochemical separation process. Bulk Ag was separated by precipitating as AgCl , by drop wise addition of 0.1 M HCl to the stock solution following the same procedure described by Maiti et al. [23]. The solution was centrifuged and filtered, and the filtrate contains only NCA ^{109}Cd radioisotope. This solution was evaporated to dryness twice, taken in 10 mL water and with this final stock solution, adsorption studies of NCA ^{109}Cd onto CA beads were performed.

Adsorption of NCA ^{109}Cd onto CA beads

The adsorptions of NCA ^{109}Cd from the aqueous solution into CA beads were examined using batch mode. Each

batch containing 30 beads of CA were exposed to 1.9 mL of HNO₃ solutions of different pH (1–5) and 0.1 mL radioactive stock solution containing ¹⁰⁹Cd. The sets were shaken and settled for 10 min each and then the beads were removed from the contact of the solutions and 1.8 mL aliquots from the supernatant were taken in eppendorf. The solutions were then assayed for γ -spectrometry of ¹⁰⁹Cd radioisotope by monitoring the characteristic photo peaks at 22.4 and 88.2 keV. The extent of adsorption was calculated from the difference in activity with a suitable standard. At the best pH condition with respect to HNO₃, shaking time, settling time and the number of beads were varied to get the optimum condition for the aforesaid extraction. The effect of bulk Cd on adsorption of NCA ¹⁰⁹Cd was also monitored. For this experiment, several sets of bulk Cd concentration (0.1, 1, 10, 30, 50 ppm) were chosen and number of beads were varied at all these bulk Cd concentrations.

Desorption

Subsequent to adsorption, study of desorption was an essential job. The desorption of NCA ¹⁰⁹Cd from CA beads was tested in different desorbing media like 0.5 M oxalic acid, 0.1 and 1 M HNO₃. A satisfactory desorption was obtained in both 0.1 and 1 M HNO₃ medium and hence desorption of bulk Cd (0.1, 1, 10, 30, 50 ppm) from CA beads was performed in 0.1 M HNO₃. The beads were found intact, with no visual degradation in its physical as well as in chemical aspect and may be reused after desorption in this medium. All the adsorption and desorption studies were carried out at 25 °C.

Adsorption isotherm modeling of Cd²⁺ ions

At the best condition of adsorption of ¹⁰⁹Cd into CA beads, (pH 4, 30 min shaking and 10 min settling time, using 50 beads) the adsorption isotherms were performed at fixed temperatures of 288, 298, 308 and 318 K and with different concentrations of Cd (0.1, 1, 10, 30, 50 ppm). 25 mL solution of each concentration was spiked with 1 mL of stock solution of NCA ¹⁰⁹Cd separately. Then all the five sets were evaporated to dryness twice and made the volume up to 25 mL with 10⁻² M HNO₃ keeping the resulting concentration same as that with the initial. 2 mL of each set of solution were treated with 50 CA beads, shaken and settled at a fixed temperature and the amount of adsorbed Cd was measured by radiometric method with the help of the characteristics photo peak of ¹⁰⁹Cd. The adsorption data was analyzed by fitting to isotherm models like Langmuir, Freundlich, Temkin and Dubinin–Radushkevich.

The Langmuir adsorption isotherm model

The Langmuir adsorption model assumes monolayer formation on the adsorbent surface. It also assumes uniform energy of adsorption and that drifting of adsorbate does not occur on surface [29]. Adsorption is assumed to occur until an equilibrium distribution of metal ions occurs between the solid and mobile phases [30]. Langmuir equation is therefore represented as:

$$q_e = \frac{q_m K_a C_e}{1 + K_a C_e} \quad (1)$$

where C_e is the equilibrium concentration of adsorbate (mg/L), q_e is the amount of metal adsorbed per gram of the adsorbent at equilibrium (mg/g), q_m is the maximum monolayer coverage capacity (mg/g), and K_a is Langmuir isotherm constant (mg/g) (L/mg)^{1/n}.

The Langmuir Eq. (1) was transformed into a linear Eq. (2) as shown below for obtaining the Langmuir adsorption parameters:

$$\frac{1}{q_e} = \frac{1}{q_m} + \frac{1}{q_m K_a C_e}. \quad (2)$$

A plot of 1/ q_e versus 1/ C_e was used for calculating the values of q_m and K_a . An essential feature of the Langmuir isotherm, the equilibrium parameter R_L (a dimensionless constant also referred to as separation factor) was calculated using Eq. 3 [31]:

$$R_L = \frac{1}{1 + (1 + K_a C_0)}. \quad (3)$$

where C_0 is the initial concentration.

The value of R_L is the indicating factor for deciding whether the adsorption process is favorable or not. It is favorable if R_L value lies between 0 and 1, linear if $R_L = 1$, irreversible if $R_L = 0$ and unfavorable if R_L is greater than 1.

The Freundlich adsorption isotherm model

This isotherm model is suitable to describe the features of those surfaces that have both homogeneous and heterogeneous features [32]. The adsorption data in such cases often fit the empirical equation proposed by Freundlich as in Eq. 4:

$$Q_e = K_f C_e^{1/n}. \quad (4)$$

where K_f is the Freundlich isotherm constant (mg/g)(L/mg)^{1/n}, n is the adsorption intensity, C_e is the equilibrium concentration of adsorbate (mg/L), and Q_e is the amount of metal adsorbed per gram of the adsorbent at equilibrium (mg/g).

Equation 4 can be further linearized as

$$\log Q_e = \log K_f + \frac{1}{n} \log C_e. \quad (5)$$

where constant K_f is a measure of the adsorption capacity at unit concentration, while $1/n$ indicates the intensity of adsorption and can be calculated from the slope and intercept respectively of the plot of $\log Q_e$ versus $\log C_e$. The partition behaviour is independent of the adsorbate concentration if $n = 1$. If $1/n < 1$ the partition behavior varies directly with the adsorbate concentration, and cooperative adsorption takes place if $1/n > 1$ [33]. Therefore $1/n$ is a heterogeneity parameter. A smaller $1/n$ value indicates greater heterogeneity and this expression reduces to a linear adsorption isotherm when $1/n = 1$. If n lies between one and ten, a favorable sorption process is predicted [34].

The Temkin adsorption isotherm model

Temkin isotherm model [35] assumes adsorbate-adsorbent interactions ignoring the extreme concentration (low and high). The heat of adsorption of all the adsorbate molecules in every layer decreases linearly with exposure to adsorbent surface. The equation is as follows [36]:

$$q_e = \frac{RT}{b} \ln(A_T C_e). \quad (6)$$

where C_e is the equilibrium concentration of adsorbate (mg/L), q_e is the amount of metal adsorbed per gram of the adsorbent at equilibrium (mg/g), A_T is Temkin isotherm equilibrium binding constant related to the maximum binding energy (L/g), b_T is Temkin isotherm constant (J/mol), R is the Universal gas constant (8.314 J/mol/K), T is the temperature (K), which is further linearized as

$$q_e = \frac{RT}{b_T} \ln A_T + \frac{RT}{b_T} \ln C_e \text{ and } q_e = B \ln A_T + B \ln C_e. \quad (7)$$

where $B = \frac{RT}{b_T}$; and is a constant related to heat of sorption (J/mol).

The derivation of the equation relies on a uniform distribution of binding energies (up to a maximum limit). The equilibrium binding constant (A_T) and the heat of adsorption (B) were calculated from the intercept and slope respectively of the q_e versus $\ln C_e$ plot.

The Dubinin–Radushkevich adsorption isotherm model

Multilayer adsorption process involving van der Waals forces of attraction are well described by the Dubinin–Radushkevich isotherm model. It involves a semi-empirical equation and is used to describe the pore filling mechanism

of the adsorbent material. This isotherm is most suitable for physical adsorption processes [37] and the linear form is represented as:

$$\ln Q_e = \ln Q_D - K_{ad} \varepsilon^2. \quad (8)$$

where Q_D is the Dubinin–Radushkevich monolayer adsorption capacity (mg/g), Q_e is the amount of metal adsorbed per gram of the adsorbent at equilibrium (mg/g), K_{ad} is Dubinin–Radushkevich isotherm constant (mol^2/kJ^2), and ε is Polanyi potential.

The model is also represented as

$$\ln Q_e = \ln Q_D - \beta \varepsilon^2 \quad (9)$$

where $\beta =$ constant related to free energy of sorption (mol^2/kJ^2).

The Polanyi potential is calculated using the Eq. 10 as

$$\varepsilon = RT \ln \left(1 + \frac{1}{C_e} \right) \quad (10)$$

where C_e is the equilibrium concentration of adsorbate (mg/L).

The values of β and Q_D were calculated from the slope and intercept of straight line plots of $\ln Q_e$ versus ε^2 respectively. A decrease in the β value with increasing temperature is associated with a decrease in adsorption capacity (Q_D) is observed.

The mean free energy of adsorption denoted by E_{D-R} (kJ/mol) is the amount of free energy produced in the system owing to transfer of 1 mol of ions from solution to the adsorbent surface and was calculated using the β values from the relationship:

$$E_{D-R} = \frac{1}{\sqrt{(-2\beta)}} \quad (11)$$

The nature of adsorption mechanism can be predicted from the value of E_{D-R} . If this value lies between 8 and 16 kJ/mol the process is designated as chemisorption, while a physical adsorption process is predicted if the values are below 8 kJ/mol [38].

Thermodynamic parameters

The mechanism of adsorption process can further be understood with the help of the thermodynamic parameters such as change in standard free energy (ΔG), enthalpy (ΔH) and entropy (ΔS).

These parameters can be determined from the following equations [39]

$$\ln K_c = -\frac{\Delta G}{RT} \quad (12)$$

$$\Delta G = \Delta H - T\Delta S \quad (13)$$

and hence

$$\ln K_c = \frac{\Delta S}{R} - \frac{\Delta H}{RT} \quad (14)$$

where R is the gas constant (8.314 J/mol K), T is the temperature (K) and K_c (L/mol) is the standard thermodynamic equilibrium constant which is calculated by

$$K_c = \frac{F_e}{1 - F_e} \quad (15)$$

Here F_e is the fractional conversion of the sorption at equilibrium and is expressed as follows

$$F_e = \frac{C_{ad}}{C_i} \quad (16)$$

C_i is the initial concentration (mg/L) of the metal ion in the solution and C_{ad} is the concentration (mg/L) of the metal ion on the adsorbent at equilibrium. All these thermodynamic parameters of our study have been obtained from the intercept and slope of $\ln K_c$ versus $1/T$ plot using the van't Hoff Eq. 14.

A positive value of ΔH reflects the endothermic nature of the process. Positive ΔS° values confirm the affinity of the adsorbent for adsorbate and increase in randomness at the interface of solid and solution during adsorption. Negative ΔG values indicate that the adsorption process is spontaneous and thermodynamically feasible [40].

Results and discussion

The present study involves the use of no-carrier-added ^{109}Cd to study the Cd uptake properties of biocompatible calcium alginate gels and to spike the bulk cadmium solutions for the adsorption isotherm experiments with the CA gels. To have an idea about the probable chemical species involved in the reactions, CHEMICAL EQUILIBRIA IN AQUATIC SYSTEMS (CHEAQS) software was used [41]. From the results it is clear that, cadmium exists as Cd^{2+} ($\sim 100\%$) in the pH range 2–5, whereas at pH 1, it exists as a mixture of Cd^{2+} (92.03%) and $\text{Cd}(\text{NO}_3)^+$ (7.77%). For the adsorption phenomenon of heavy metals onto adsorbent materials, pH takes a decisive role as shown in Fig. 1. The figure illustrates that the adsorption is more or less same in the range of pH 3–5, slightly decreases at pH 2, and falls very sharply at pH 1. This is presumably because of the pK_a value of the carboxylic acids which lies in the range 3–5 and a considerable amount of free carboxylate ions are present in this pH range which is also indicated by the Henderson–Hasselbalch equation. Therefore strong electrostatic attractions and van der Waals forces come into play between COO^- group and Cd^{2+} metal ion. Additionally, cationic exchange between Cd^{2+} and Ca^{2+} in CA beads also has a large impact on the adsorption and hence

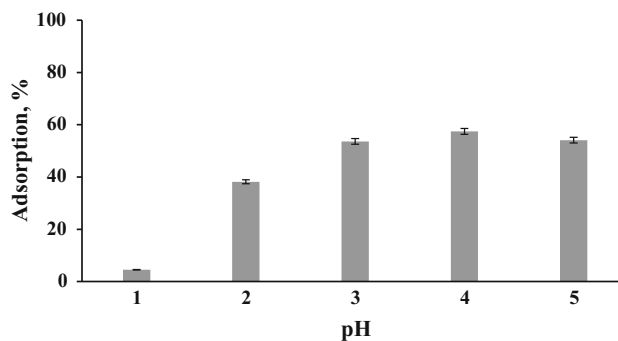


Fig. 1 Adsorption profile of NCA ^{109}Cd onto CA beads with varying pH of HNO_3 medium, (with 30 beads, 10 min shaking and 10 min settling time)

greater adsorption percentage ($\sim 60\%$, at pH 4) was found. But at the lower pH (1,2) COO^- group gets protonated [42] and due to excessive protonation of active sites, surface of adsorbent (CA) becomes positively charged which repels the entering Cd^{2+} along with a competition between H_3O^+ and Cd^{2+} for binding sites resulting in a smaller extent of adsorption of Cd^{2+} into the CA matrix.

To obtain better adsorption, contact time (including shaking and settling) of CA beads with aqueous Cd^{2+} solution were varied. The results are shown in Fig. 2. Adsorption percentage increased with increasing shaking time up to 30 min and became static after this. No significant change in adsorption was obtained with varying the range of settling time. The numbers of beads were then varied. Figure 3 shows that the number of binding sites available was large enough to bind NCA Cd^{2+} at all the experimental conditions and hence any significant change in the adsorption was not observed. An optimum condition was obtained at pH 4, shaking time 30 min and settling time 10 min and 50 CA beads, when around 87% NCA Cd^{2+} was adsorbed.

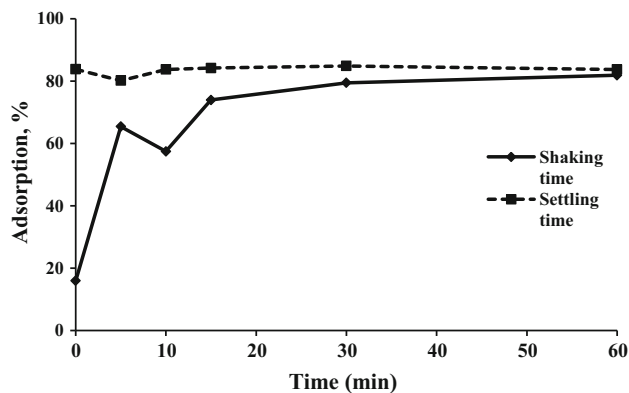


Fig. 2 Adsorption profile of NCA ^{109}Cd onto 30 CA beads with variation of shaking and settling time at pH 4 of HNO_3 medium

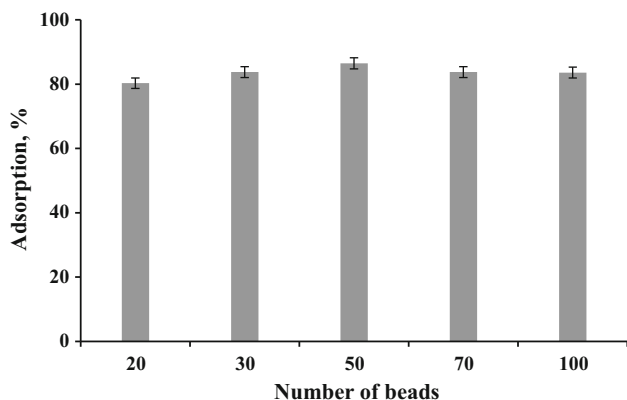
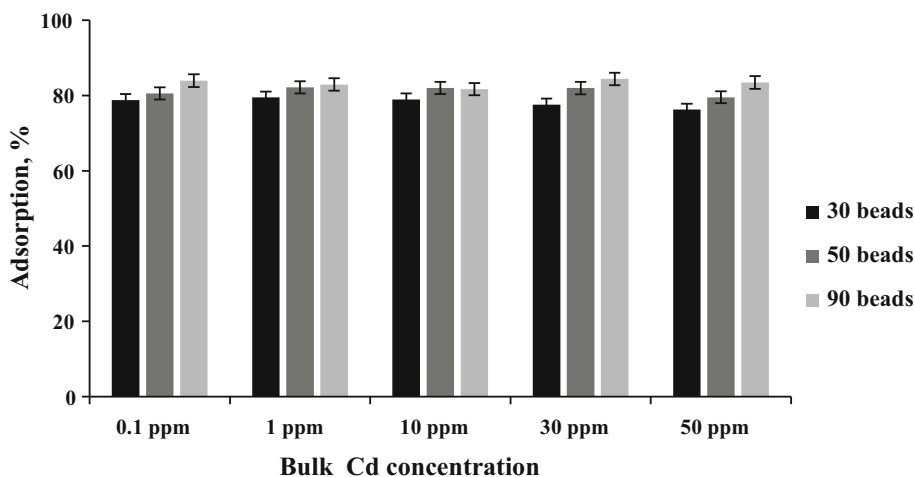


Fig. 3 Adsorption profile of NCA¹⁰⁹Cd onto varying number of CA beads at pH 4 of HNO₃ medium (30 min shaking and 10 min settling time)

Now, we tried to find the adsorption capability of bulk metallic cadmium into CA beads. A new experimental set was designed with a wide range of bulk Cd²⁺ (0.1–50 ppm) solution spiked with NCA ¹⁰⁹Cd to monitor the adsorption using radiometric method via the characteristic photo-peaks of ¹⁰⁹Cd at 22.4 and 88.2 keV. The number of CA beads were varied (30, 50, 90) in this concentration range. At all the concentrations, adsorption was found to be more or less equal and lies in the range 80–85% in each set of experiment (Fig. 4). It implies that the number of beads in our experiment was sufficient to adsorb a satisfactory amount of bulk Cd²⁺ and consequently adsorption isotherm experiment was performed with 50 CA beads at pH 4, shaking time 30 min and settling time 10 min.

Desorption of NCA ¹⁰⁹Cd from CA beads was then performed in different desorbing media such as 0.5 M oxalic acid, 0.1 and 1 M HNO₃ (Fig. 5). ~10% NCA ¹⁰⁹Cd was desorbed in 0.5 M oxalic acid, whereas ~92% of the same was desorbed in both 0.1 and 1 M HNO₃ media

Fig. 4 Adsorption profile of NCA¹⁰⁹Cd onto different number of CA beads at pH 4 of HNO₃ medium in presence of different bulk Cd concentration (30 min shaking and 10 min settling time)



as it offers a strong acidic condition. As both the 0.1 and 1 M HNO₃ media are equally capable towards desorption, we chose 0.1 M HNO₃ avoiding higher acid concentration for bulk Cd²⁺ removal. Figure 6 shows that ~95% bulk Cd²⁺ was desorbed successfully in 0.1 M HNO₃ medium at all the bulk concentrations.

The Langmuir constants q_m and K_L (which is also represented as b in linear form of Langmuir) were obtained from the slope and intercept of $1/q_e$ vs. $1/C_e$ plot obtained from linearized form of non-linear Langmuir equation shown in Fig. 7 and the Langmuir isotherm parameters are tabulated in Table 1. The maximum adsorption capacities (q_m) of Cd²⁺ by the CA were 4.92, 2.42, 2.48, 8.09, mg/g calculated from non-linear Langmuir equation at 288, 298, 308 and 318 K respectively. The regression coefficient (R^2) values 0.998, 0.999, 0.998, 0.999 at the experimental temperatures show that the data were fitted very well in this method and the adsorption process could be described by the Langmuir equation which indicates a homogeneous monolayer adsorption process. The constant K_L expresses the affinity between the adsorbent and adsorbate [43] and a low value of K_L (0.0076–0.026) obtained from our experimental results indicated that CA beads have a high affinity for Cd²⁺ ion. Finally, the values of equilibrium parameter (R_L) at all the experimental temperatures and all the starting concentrations lie between $0 < R_L < 1$ which indicates that the adsorption process is very much favorable.

Figure 8 shows the plot of $\log Q_e$ versus $\log C_e$ obtained from linear Freundlich equation and the isotherm parameters n and K_f were obtained from the slope and intercept respectively and are given in Table 1. As all the n values are found to be ~1, it implies a beneficial adsorption phenomenon as according to Kadirvelu and Namasivayam [44], the n values lying in the range 1–10 indicates adsorption processes independent of the initial concentration. The n value also indicates that the CA bead has a high

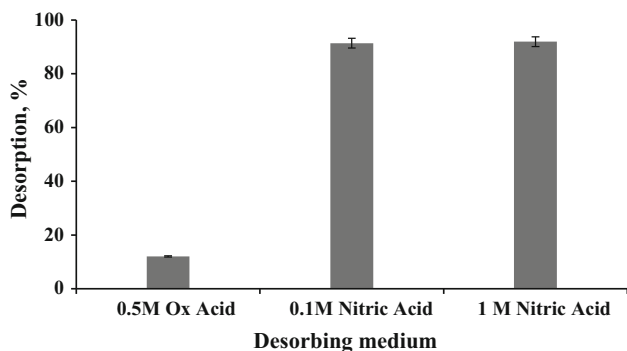


Fig. 5 Desorption profile of NCA¹⁰⁹Cd from CA beads in different desorbing media

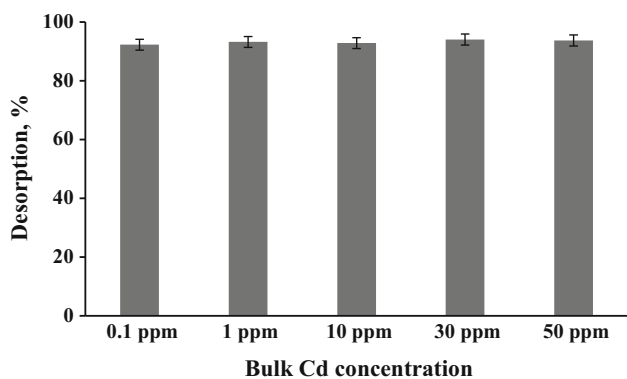
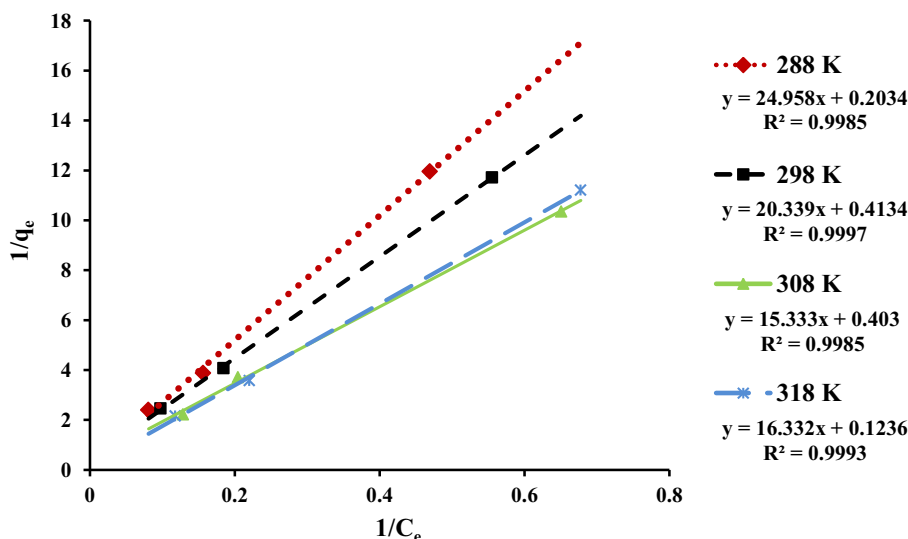


Fig. 6 Desorption of bulk Cd of different concentrations from CA beads in 0.1 M HNO₃

affinity for Cd²⁺ ions in solution and a heterogeneous adsorption is expected. Maximum adsorption capacity (q_m) were calculated with the help of K_f values and 50 ppm as the initial concentration at all the temperatures and were found to be 1.80, 2.19, 2.80, 2.77 mg/g for 288, 298, 308 and 318 K respectively. The regression coefficient (R^2)

Fig. 7 Langmuir adsorption isotherm plots



value was 0.999 for all the set of data, which implies excellent fitting of the experimental data, thus obey the Freundlich isotherm and a multilayer adsorption process is expected [45].

Temkin isotherm model was applied by a linear plot of q_e against $\ln C_e$ shown in Fig. 9, the constants B and A_T were calculated from the slope and intercept respectively and Temkin isotherm constants (b_T) were calculated from B values. The Temkin isotherm parameters A , B , b_T and R^2 are presented in Table 1. The magnitudes of A_T (15.66, 16.47, 22.10, 21.68 L/g) and b_T (41.43, 43.09, 41.57, 40.49 kJ/mole) at 288, 298, 308, 318 K respectively were high which indicates a very strong interaction of Cd²⁺ with CA beads and therefore, the process might be chemisorption along with the physical adsorption. Again, the regression coefficient (R^2) value was ~ 0.7 for all the set of data and shows a weaker fitting of the data as well as applicability of this isotherm model as compared to the Langmuir and Freundlich models.

The values of β and Q_D were calculated from the slope and intercept of straight line plots of $\ln Q_e$ versus ε^2 following the Dubinin–Radushkevich isotherm model represented in Fig. 10. Then the mean free energy of adsorption (E_{D-R}) was calculated from β values and all the isotherm parameters are summarized in Table 1. The Q_D values were 7.159, 7.159, 6.486, 6.497 mg/g at 288, 298, 308, 318 K respectively and matches with the non-linear Langmuir isotherm. E_{D-R} values were calculated as 2.837, 2.957, 3.30 and 3.43 kJ/mol and the adsorption process is designated to be predominated by physical adsorption as compared to chemical interactions. The values of regression coefficient (R^2) were ~ 0.84 for all sets of data which indicates that this isotherm did not provided a very good fit to the experimental data, though it is slightly higher than that of Temkin adsorption isotherm.

Table 1 Isotherm model parameters and coefficient of determination (R^2) for cadmium adsorption by CA beads at different temperatures

Langmuir adsorption isotherm					Freundlich adsorption isotherm				
T (K)	q_m (mg/g)	K_L (mg/g) (mg/L) ^{1/n}	R_L^a	R^2	q_m^a (mg/g)	K_f (mg/g) (mg/L) ^{1/n}	N	R^2	
288	4.92	0.008	0.71	0.998	1.80	0.03961	1.03	0.998	
298	2.42	0.020	0.50	0.999	2.19	0.0438	0.99	0.999	
308	2.48	0.026	0.43	0.998	2.80	0.05913	1.01	0.999	
318	8.09	0.008	0.72	0.999	2.77	0.0598	1.02	0.999	

Temkin adsorption isotherm					Dubinin–Radushkevich adsorption isotherm			
T (K)	A_T (L/g)	B (J/mol)	b_T (kJ/mol)	R^2	Q_D (mg/g)	β (mol ² /kJ ²)	E_{D-R} (kJ/mol)	R^2
288	15.66	0.0578	41.43	0.734	7.159	-0.0621	2.84	0.837
298	16.47	0.0575	43.09	0.738	7.159	-0.0574	2.96	0.841
308	22.10	0.0616	41.57	0.714	6.486	-0.0459	3.30	0.839
318	21.68	0.0653	40.49	0.717	6.497	-0.0426	3.43	0.832

^a Shows the R_L (Langmuir) and q_m (Freundlich) value calculated at 50 ppm (50.022 mg/L) initial metal ions concentration

Fig. 8 Freundlich adsorption isotherm plots

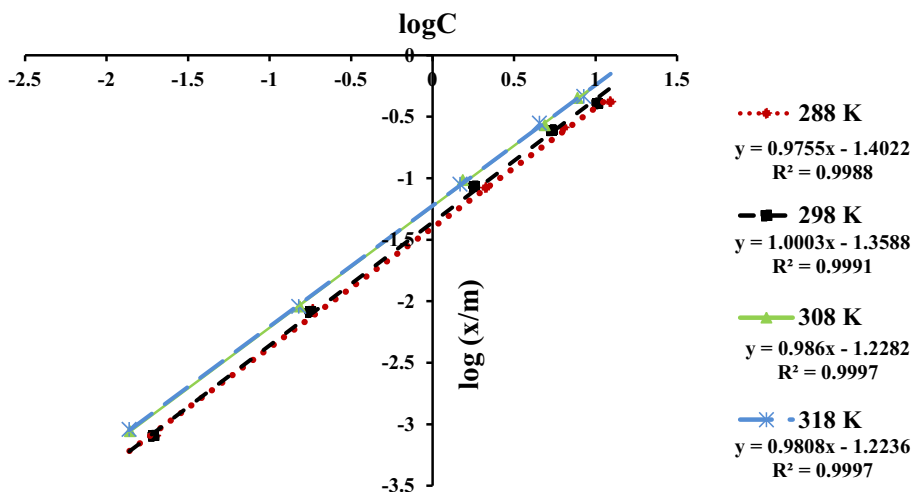


Fig. 9 Temkin adsorption isotherm plots

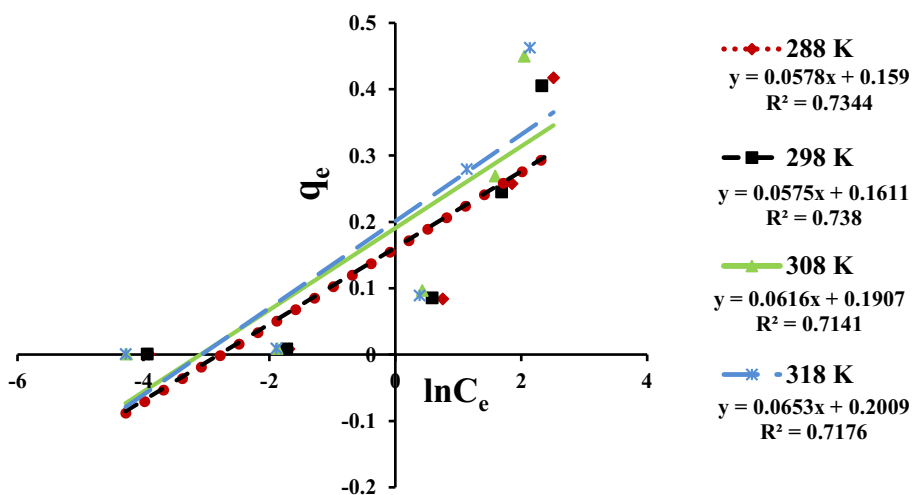
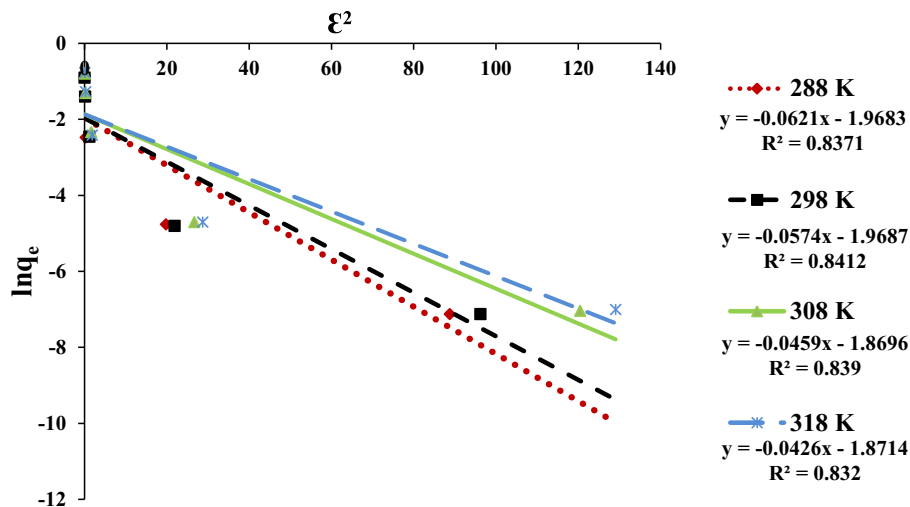


Fig. 10 Dubinin–Radushkevich isotherm plots



The values of some thermodynamic parameters like ΔH and ΔS were calculated from the slopes and intercepts of the plots of $\ln K_c$ as a function of $1/T$ for different Cd^{2+} concentrations and are shown in Fig. 11. Then the change in free energy (ΔG) was calculated from $\ln K_c$ values and all the thermodynamic parameters are tabulated in Table 2. The negative values of Gibbs free energy (ΔG) of the interactions for all the sets of data (in the range of -3 to -5) demonstrate that the process is spontaneous, feasible and favorable towards formation of electrostatic interaction between Cd^{2+} –CA beads [46]. Zhang et al. [47] reported that the change in enthalpy (ΔH) should be lower than that of 20.0 kJ/mol for physical adsorption. The ΔH values of our experiments were found positive, and numerical values were 13.30, 6.86, 11.79, 10.59 and 13.63 kJ/mol for 0.1, 1, 10, 30 and 50 ppm initial concentration of Cd^{2+} metal ion respectively indicating the physical adsorption of Cd^{2+} onto CA beads. These positive values of ΔH also demonstrate the endothermic nature of the process involving weak interactions. Again, the high positive values of ΔS , i.e.,

57.40, 36.04, 52.05, 47.86 and 56.99 J/mol K for 0.1, 1, 10, 30 and 50 ppm initial concentration of Cd^{2+} metal ion respectively indicate the increase in the degree of freedom of the adsorbing system with spontaneity and higher randomness of the metal ions near the adsorbent surface during the sorption process.

There are numerous reports on adsorption of Cd^{2+} in bare CA beads [48, 49] and modified CA beads [50–53] in the literature. Some of them report better results while the others are comparable with the present study. However, most of the reports have certain limitations in the experimental procedure as well as in the detection methods. Several of them suffer from low adsorption capacity at high Cd^{2+} concentration and high pH even after a long contact time [54, 55] and with high adsorbent dosage [56]. Some others have low adsorption capacity in the acidic pH range [57, 58] and at higher temperatures [59]. In contrast, our method is capable to work in a very wide range of metal ion concentrations (0.1–50 ppm) and shows high adsorption capacity in a wide pH range (2–5) even with low

Fig. 11 The plot of $\ln K_c$ versus $1/T$ for obtaining thermodynamic parameters

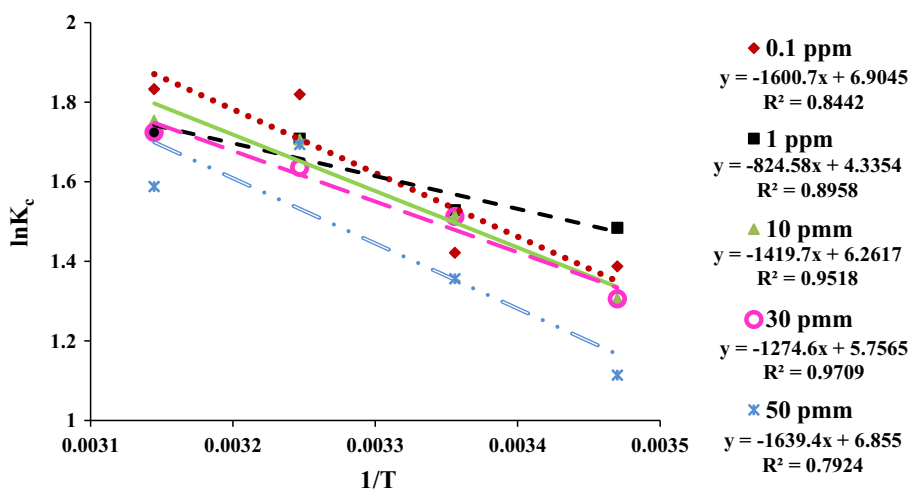


Table 2 Thermodynamic parameters for adsorption of Cd²⁺ ions from aqueous solutions onto the CA beads

Cd ²⁺ concentration	Temperature (K)	ΔG (kJ/mol)	ΔH (kJ/mol)	ΔS (J/mol K)
0.1 ppm	288	-3.32	13.30	57.40
	298	-3.52		
	308	-4.66		
	318	-4.85		
1 ppm	288	-3.55	6.86	36.04
	298	-3.79		
	308	-4.37		
	318	-4.55		
10 ppm	288	-3.13	11.79	52.05
	298	-3.76		
	308	-4.37		
	318	-4.64		
30 ppm	288	-3.13	10.59	47.86
	298	-3.75		
	308	-4.19		
	318	-4.56		
50 ppm	288	-2.67	13.63	56.99
	298	-4.49		
	308	-4.34		
	318	-4.20		

contact time and lesser amount of adsorbent. Additionally, the sensitivity of our detection method is better over other methods as we have used radiometry using NCA radionuclides for the studies of adsorption isotherm phenomena.

Conclusion

CA beads were used for the adsorption studies of radio-pharmaceutically important NCA ¹⁰⁹Cd radioisotope from bulk free aqueous solution with a high efficiency. The capacity of CA beads for high concentration of bulk Cd²⁺ adsorption was also examined with the help of radiometric method. Adsorption capability of environmentally hazardous, toxic and carcinogenic bulk Cd²⁺ was in agreement with that in NCA scale and hence the adsorption isotherm experiment was performed and our experimental data were excellently fitted to both non-linear Langmuir and linear Freundlich adsorption isotherm equations followed by Dubinin–Radushkevich and then Temkin isotherm models. With the isotherm data, all the thermodynamic parameters were calculated and it can be concluded that the adsorption process is monolayer as well as multilayer and it is a heterogeneous physisorption process predominating over the chemisorptions. In addition, it is a spontaneous endothermic process which suggests a high feasibility of the adsorption process involving electrostatic as well as van der Waal's interactions.

Acknowledgement One of the authors gratefully acknowledges the University Grants Commission (UGC) for providing necessary fellowship. This work is a part of SINP-DAE 12 Five years plan project Trace and Ultratrace Analysis and Isotope Production (TULIP).

References

1. Vis RD, Bos AJJ, Idzenga S, Verheul H (1979) Perturbed γ - γ angular correlations of ^{111m}Cd bound on DNA. Nucl Inst Meth 163:265–267
2. Das SK, Guin R, Banerjee D, Johnston K, Das P, Butz T, Amaral VS, Correia JG, Barbosa MB (2014) Perturbed angular correlation study of the static and dynamic aspects of cadmium and mercury atoms inside and attached to a C60 fullerene cage. Z Naturforsch A 69:611–618
3. Goetz L, Sabbioni E, Marafante E, Birattari C, Bonardi M (1980) Cyclotron production of ^{107,109}Cd for use in metallobiochemistry of heavy metal pollution. Radiochem Radioanal Lett 45:51
4. Lahiri S, Mukhopadhyay B, Nandy M, Das NR (1997) Sequential separation by HDEHP of carrier-free ^{101,105,106}Rh, ^{103,104,105,106,110,112}Ag and ^{104,105,107,109,111}Cd produced in alpha particle activated palladium. J Radioanal Nucl Chem 224:155–158
5. Long X, Peng X, Fuqing H, Mantian L (1991) Production of cadmium-107 and cadmium-109 by deuteron bombardment of silver. Int J Appl Radiat Isot 42:1234–1236
6. Peng X, Xianguan L, He F, Li M (1992) Excitation function for ¹⁰⁷Ag(d,2n)¹⁰⁷Cd, ¹⁰⁹Ag(d,2n)¹⁰⁹Cd and ¹⁰⁹Ag(d, p)^{110m}Ag reactions. Nucl Instrum Meth B 68:145–148
7. Aardaneh K, Naidoo C, Steyn GF (2008) Radiochemical separation of ¹⁰⁹Cd from a silver target, J Radioanal. Nucl Chem 276:831–834

8. Xue Z, Rehkämper M, Schönbächler M, Statham PJ, Coles BJ (2012) A new methodology for precise cadmium isotope analyses of seawater. *Anal Bioanal Chem* 402:883–893
9. Zhu C, Wen H, Zhang Y, Fu S, Fan H, Cloquet C (2016) Cadmium isotope fractionation in the Fule Mississippi Valley-type deposit, Southwest China. *Miner Depos*. doi:10.1007/s00126-016-0691-7
10. Krishnamurthy N (2013) *Engg. chemistry*, 2nd edn. PHI Learning Private Limited, New York, pp 82–83. ISBN 978-81-203-3666-7
11. Marder L, Bernardes AM, Ferreira JZ (2004) Cadmium electroplating wastewater treatment using a laboratory-scale electro-dialysis system. *Sep Purif Technol* 37:247–255
12. Scoullos Michael J, Vonkeman Gerrit H, Iain Thornton, Zen Makuch (2001) Mercury, cadmium, lead. *Handbook for sustainable heavy metals policy and regulation*. Springer, New York. ISBN 978-1-4020-0224-3
13. Bezerra MA, Maêda SMN, Oliveiraa EP, Carvalhoc MD, Santellia RE (2007) Internal standardization for the determination of cadmium, cobalt, chromium and manganese in saline produced water from petroleum industry by inductively coupled plasma optical emission spectrometry after cloud point extraction. *Spect. Acta Part B: At Spectrosc* 62:985–991
14. Adeniyi AA, Afolabi JA (2002) Determination of total petroleum hydrocarbons and heavy metals in soils within the vicinity of facilities handling refined petroleum products in Lagos metropolis. *Environ Int* 28:79–82
15. Bernard A (2008) Cadmium & its adverse effects on human health. *Indian J Med Res* 128:557–564
16. Agency for Toxic Substances and Disease Registry (ATSDR) (1997) Toxicological profile for cadmium. Draft for public comment. Public Health Service, US Department of Health and Human Services, Atlanta
17. Calabrese EJ, Kenyon EM (1991) *Air toxics and risk assessment*. Lewis Publishers, Chelsea
18. US Department of Health and Human Services. Hazardous Substances Data Bank (HSDB, online database). (1993) National toxicology information program, National Library of Medicine, Bethesda
19. Maiti M, Ghosh K, Lahiri S (2015) Green methods for the radiochemical separations of no-carrier added ^{61}Cu , ^{62}Zn from ^7Li irradiated cobalt target. *J Radioanal Nucl Chem* 303:2033–2040
20. Fuks L, Oszczak A, Gniazdowska E, Sternik D (2015) Calcium alginate and chitosan as potential sorbents for strontium radionuclide. *J Radioanal Nucl Chem* 304:15–20
21. Fadl FIAE (2014) Radiation grafting of ionically crosslinked alginate/chitosan beads with acrylic acid for lead sorption. *J Radioanal Nucl Chem* 301:529–535
22. Yagnesh L, Patel PS, Atmaram PP (2006) The effect of drug concentration and curing time on processing and properties of calcium alginate beads containing metronidazole by response surface methodology. *AAPS PharmSciTech* 7(4):E1–E7
23. Maiti M, Lahiri S, Tomar BS (2011) Separation of no-carrier-added $^{107,109}\text{Cd}$ from proton induced silver target: classical chemistry still relevant. *J Radioanal Nucl Chem* 288:115–119
24. Ghosh K, Maiti M, Lahiri S, Afzal Hussain (2014) Ionic liquid-salt based aqueous biphasic system for separation of ^{109}Cd from silver target. *J Radioanal Nucl Chem* 302:925–930
25. Maiti M, Ghosh K, Lahiri S (2013) Simultaneous production and separation of no-carrier-added ^{111}In , ^{109}Cd from alpha particle induced silver target. *J Radioanal Nucl Chem* 295:1945–1950
26. Sarkar K, Ansari Z, Sen K (2016) Detoxification of Hg(II) from aqueous and enzyme media: pristine vs. tailored calcium alginate hydrogels. *Int J Biol Macromol* 91:165–173
27. Sarkar K, Sen K (2015) On the design of Ag-morinnanocomposite to modify calcium alginate gel: framing out a novel sodium ion trap. *RSC Adv*. 5:57223–57230
28. Mondal A, Lahiri S (2011) Separation of ^{134}Cs and ^{133}Ba radionuclides by calcium alginate beads. *J Radioanal Nucl Chem* 290:115–118
29. Sharma YC, Srivastava V, Upadhyay SN, Weng CH (2008) Alumina nanoparticles for the removal of Ni(II) from aqueous solutions. *Ind Eng Chem Res* 47:8095–8100
30. Vermeulan TH, Vermeulan KR, Hall LC (1966) *Fundamental*. *Ind Eng Chem* 5:212–223
31. Dada AO, Olalekan AP, Olatunya A, Dada O (2012) Langmuir, Freundlich, Temkin and Dubinin–Radushkevich isotherms studies of equilibrium sorption of Zn^{2+} onto phosphoric acid modified rice husk. *IOSR-JAC* 3:38–45
32. Hutson ND, Yang RT (2000) Adsorption. *J Colloid Interf Sci* p 189
33. Mohan S, Karthikeyan J (1997) Removal of lignin and tannin color from aqueous solution by adsorption on to activated carbon solution by adsorption on to activated charcoal. *Environ Pollut* 97:183–187
34. Goldberg S (2005) “Equations and models describing adsorption processes in soils”. *Soil Science Society of America*, 677 S. Segoe Road, Madison, WI 53711, USA. Chemical processes in soils. SSSA book series, no. 8
35. Temkin MJ, Pyzhev V (1940) Recent modifications to Langmuir isotherms. *Acta Phys chim. URSS* 12:217–225
36. Khan TA, Chaudhry SA, Ali I (2015) Equilibrium uptake, isotherm and kinetic studies of Cd(II) adsorption onto iron oxide activated red mud from aqueous solution. *J Mol Liq* 202:165–175
37. Hutson ND, Yang RT (1997) Theoretical basis for the Dubinin–Radushkevitch (D–R) adsorption isotherm equation. *Adsorption* 3:189–195
38. Dawodu FA, Akpomie GK, Ogbu IC (2012) Isotherm modeling on the equilibrium sorption of cadmium(II) from solution by Agbani clay. *Int. J. Multidiscip. Sc. Eng.* 3:9–14
39. Villanueva RAC, Vázquez ARH, de Jesús Cortés Penagos C, Martínez RC (2014) Thermodynamic, kinetic, and equilibrium parameters for the removal of lead and cadmium from aqueous solutions with calcium alginate beads. *Sci World J*. doi:10.1155/2014/647512
40. Bayramoglu G, Arica MY (2011) Preparation of a composite biosorbent using *Scenedesmus quadricauda* biomass and alginate/polyvinyl alcohol for removal of Cu(II) and Cd(II) ions: isotherms kinetics, and thermodynamic studies. *Water Air Soil Pollut* 221:391–403
41. Verweij W (2005) ‘CHEAQS PRO’: a program for calculating chemical equilibria in aquatic systems’. <http://home.tiscali.nl/cheaqs/>. Accessed 25 Oct 2016
42. Wang F, Lua X, Lia XY (2016) Selective removals of heavy metals (Pb^{2+} , Cu^{2+} , and Cd^{2+}) from waste water by gelation with alginate for effective metal recovery. *J Hazard Mater* 308:75–83
43. Vijayaraghavan K, Jegan JR, Palanivelu K, Velan M (2005) Nickel recovery from aqueous solution using crab shell particles”. *Adsorpt Sci Technol* 23:303–311
44. Kadirvelu K, Namasivayan C (2003) Utilization of various agricultural waste for activated carbon preparation and application for the removal of dyes and metal ions from aqueous. *Bioresour Technol* 87:129–132
45. Chowdhury ZZ, Zain SM, Khan RA, Khalid K (2011) Linear regression analysis for kinetics and isotherm studies of sorption of manganese(II) ions onto activated palm ash from waste water. *Orient J Chem* 27:405–415
46. Bayramoglu G, Arica MY (2009) Construction a hybrid biosorbent using *Scenedesmus quadricauda* and Ca alginate for biosorption of Cu(II), Zn(II) and Ni(II): kinetics and equilibrium studies. *Bioresour Technol* 100:186–193
47. Zhang F, Jin Q, Chan SW (2004) Ceria nanoparticles: size, size distribution, and shape. *J Appl Phys* 95:4319–4325

48. Papageorgiou SK, Kouvelos EP, Katsaros FK (2008) Calcium alginate beads from *Laminariadigitata* for the removal of Cu^{+2} and Cd^{+2} from dilute aqueous metal solutions. *Desalination* 224:293–306
49. Niță I, Iorgulescu M, Spiroiu MF, Ghiurea M, Petcu C, Cintează O (2007) The adsorption of heavy metal ions on porous calcium alginate microparticles. *Analele Universității din București—Chimie, Anul XVI (serienouă)* 1:59–67
50. Bayramoğlu G, Tuzun I, Celik G, Yilmaz M, Arica MY (2006) Biosorption of mercury(II), cadmium(II) and lead(II) ions from aqueous system by microalgae *Chlamydomonasreinhardtii* immobilized in alginate beads. *Int J Miner Process* 81:35–43
51. Ozdemir G, Ceyhan N, Manav E (2005) Utilization of an exopolysaccharide produced by *Chryseomonasluteola* TEM05 in alginate beads for adsorption of cadmium and cobalt ions. *Bioresour Technol* 96:1677–1682
52. Cataldo S, Cavallaro G, Gianguzza A, Lazzara G, Pettignano A, Piazzese D, Villaescusa I (2013) Kinetic and equilibrium study for cadmium and copper removal from aqueous solutions by sorption onto mixed alginate/pectin gel beads. *J Environ Chem Eng* 1:1252–1260
53. Jain M, Garg VK, Kadirvelu K (2013) Cadmium(II) sorption and desorption in a fixed bed column using sunflower waste carbon calcium–alginate beads. *Bioresour Technol* 129:242–248
54. Basso MC, Cerrella EG, Cukierman AL (2002) Activated carbons developed from a rapidly renewable biosource for removal of cadmium(II) and nickel(II) ions from dilute aqueous solutions. *Ind Eng Chem Res* 41:180–189
55. Debnath S, Nandi D, Ghosh UC (2011) Adsorption–desorption behavior of cadmium(II) and copper(II) on the surface of nanoparticle agglomerates of hydrous titanium(IV) oxide. *J Chem Eng Data* 56:3021–3028
56. Luo X, Guo B, Wang L, Deng F, Qi R, Luo S, Au C (2014) Synthesis of magnetic ion imprinted fluorescent CdTe quantum dots by chemical etching and their visualization application for selective removal of Cd(II) from water. *Colloids Surf A* 462:186–193
57. Repo E, Warchol JK, Bhatnagar A, Sillanpa M (2011) Heavy metals adsorption by novel EDTA-modified chitosan–silica hybrid materials. *J Colloid Interface Sci* 358:261–267
58. Khan TA, Singh VV, Ali I (2009) Sorption of Cd(II), Pb(II) and Cr(VI) metal ions from wastewater using bottom fly ash as a low cost sorbent. *J Environ Prot Sci* 3:124–132
59. Khan TA, Singh VV (2010) Removal of cadmium(II), lead(II), and Chromium(VI) ions from aqueous solution using clay. *Toxicol Environ Chem* 92:1435–1446